

# Analysis of deformation characteristic in multi-way loading forming process of aluminum alloy cross valve based on finite element model

Da-wei ZHANG<sup>1</sup>, Sheng-dun ZHAO<sup>1</sup>, He YANG<sup>2</sup>

1. School of Mechanical Engineering, Xi'an Jiaotong University, Xi'an 710049, China;

2. School of Materials Science and Engineering, Northwestern Polytechnical University, Xi'an 710072, China

Received 31 December 2012; accepted 10 April 2013

**Abstract:** The deformation characteristic in the forming process of aluminum alloy 7075 cross valve under multi-way loading was investigated by numerical simulation method. The results indicate that there exist 4 deformation patterns in the multi-way loading forming process of cross valve, such as forward extrusion, backward extrusion, forward-lateral extrusion and backward-lateral extrusion; one or several patterns occur at different forming stages depending on loading path. In general, the main deformation pattern is forward extrusion or backward extrusion at the initial stage; the main deformation pattern is backward extrusion at the intermediate stage, and the backward extrusion and forward-lateral extrusion occur at the final stage. In order to improve the cavity fill and reduce the forming defects, the lateral extrusion deformation should be increased at the initial and intermediate stages, and the forward extrusion deformation at the final forging stage should be reduced or avoided.

**Key words:** cross valve; multi-way loading; deformation behavior; metal flow; aluminum alloy; FEM; numerical simulation

## 1 Introduction

The traditional method of plastic processing of a multi-ported valve is multi-pass die forging with flash, which includes multi heating and flash cutting and is characterized by low efficiency and large material loss [1,2]. This traditional method is difficult to meet the manufacture of high strength and high precision complex valve used light-weight and hard-working materials such as aluminum alloy 7075. The multi-way loading forming process, in which dies could be loaded in multi-direction at the same time or in sequential time in one working cycle, provides an efficient approach to near-net shape form this component [3].

With extensive progresses in computer aided engineering and computer technology, finite element method (FEM) numerical simulation has been widely used in analyzing, predicting and controlling of plastic forming process, and has become a powerful approach for investigating and developing of advanced plastic processing technologies [4,5]. FEM numerical simulation can provide a clear stress, strain and temperature distribution, microstructure evolution, and defects

development during the forming process [6–8], and it is best suited for analyzing forming process, exploring forming characteristic, and optimizing processing parameters with low cost and short cycle [9–11]. Thus, numerical simulation method is also an important way to investigate the multi-way loading forming process.

GONTARZ [2] carried out a physical modeling experiment and the FEM numerical simulation of forming process of valve drop forging with three cavities. It was found that the magnitude of strain has significant influence on forming quality and work done according to the FEM results. GUO et al [12] studied the multi-way forging process of the blade with a damper platform by FEM, and explored the field-variable distribution laws. Using FEM numerical simulation, SUN et al [13] researched the forming load, distribution of temperature field, and microstructure evolution in the multi-way loading forming process of AISI 5140 steel triple valve.

CHENG and ZHANG [14] investigated the metal flow during triple valve multi-way loading forming process by FEM numerical simulation. It was presented that the metal flow was influenced by loading sequence. The forming process between triple valve and cross valve was compared using the numerical simulation

method by ZHANG et al [15]. It was presented that there existed similar laws for load in the processes of triple valve and cross valve under similar loading paths but the metal flows were different under different loading paths. XU [16] studied the multi-ram forging of triple valve and presented that there existed backward extrusion, lateral extrusion and their combination. However, in multi-way loading forming process of cross valve, ZHANG et al [3] reported that the forward extrusion and forward-lateral extrusion may exist besides the deformation patterns declared by XU [16].

Up to now, most research is focused on triple valve multi-way loading forming, and few studies are done on integral forging of cross valve by multi-way loading. ZHANG et al [17] investigated the cross valve multi-way loading forming process using thermo-mechanical coupled finite element method. It was presented that the laws between non-isothermal process simulation and isothermal process simulation were similar but the magnitudes of these were more different, and the distributions of strain and temperature fields between two typical loading paths were more different. Further study indicated that the final deformation between two loading paths had a little difference but the load and damage had a notable difference [18].

Thus, in this work, based on the two typical loading paths used in Refs [17,18], the deformation characteristic in multi-way loading process of aluminum alloy 7075 cross valve is investigated by thermo-mechanical coupled finite element method. The influences of loading condition on deformation pattern, load and cavity fill are analyzed. The results indicate that the deformation behavior discrepancy is the essential reason for forming difference caused by different loading paths. The discrepancy of deformation patterns at different forming stage results in different metal flow, and finally the differences of cavity fill, forging load and field variables evolution are shown.

## 2 Finite element analysis

### 2.1 Multi-way loading process

In the present study, the multi-way loading process of cross valve is a flashless die forging, which includes 6 dies such as 2 female dies and 4 male dies. During the multi-way loading process, upper and lower ( $z$  axis) female dies are closed firstly, and then the male dies in the plane ( $x$  and  $y$  axis) are loaded at the same time or in sequential time, finally the cross valve can be manufactured in one working cycle. There are two loading methods for valve body multi-way loading forming: loading in sequential time and loading at the same time. The folding/lap defect is prone to occurrence under loading in sequential time and can be avoided

under loading at the same time [15].

The loading method of loading at the same time for forming cross valve can be realized by two typical loading paths [17,18], as shown in Fig. 1. Figure 1(a) shows the loading path I which puts the billet along  $x$  axis. The  $y$  axial protrusion is formed via lateral extrusion at the initial forming stage, and the  $y$  axial cavity is formed via lateral and backward extrusion. Figure 1(b) shows the loading path II which puts the billet along  $y$  axis. The  $x$  axial cavity is formed via backward and lateral extrusion. The evolutions of field variables and forging load under different loading speeds of male die are similar but the magnitudes are different [18].

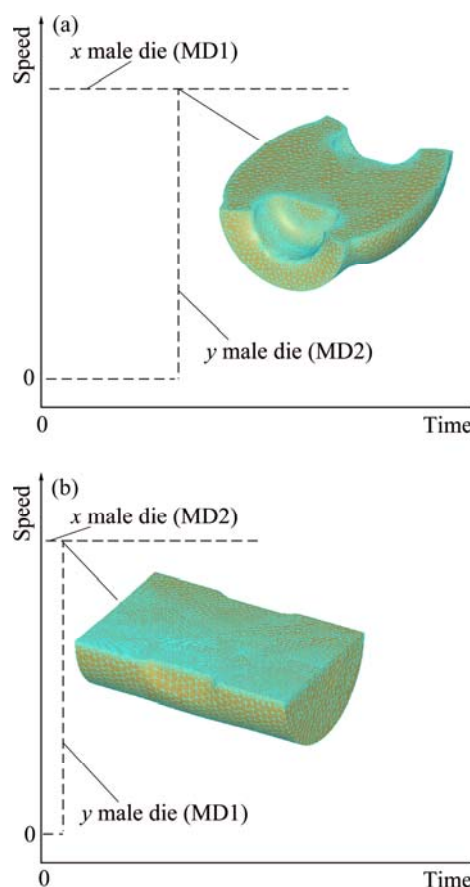


**Fig. 1** Speed-time curve of male dies: (a) Loading path I; (b) Loading path II

### 2.2 FEM simulation

Based on finite element soft environment of DFEORM-3D, a coupled thermal-mechanical finite element model of multi-way loading forming process of multi-ported valve body has been established, and the model has been verified with respect to geometry development and forming defect [15]. Then, the 3D finite element model of multi-way loading process of aluminum alloy cross valve has been used in Ref. [17]. Thus, based on the validated finite element model, the numerical simulation results in this work can be

considered to be valid. Table 1 lists the parameters used in the numerical simulations [17].

**Table 1** Parameters of FEM numerical simulation

Parameter	Value
Temperature of room/°C	20
Diameter of billet/mm	50
Length of billet/mm	75
Initial temperature of billet/°C	450
Initial temperature of die/°C	400
Coefficient of friction	0.4
Loading speed of male die/(mm·s <sup>-1</sup> )	10

### 2.3 Analysis of cross valve forming

The male dies can be classified into two categories according to the relationship between the axial line of initial billet and the axial line of male die: 1) the axial line of male die is parallel to the axial line of initial billet, and this male die is marked as MD1; 2) the axial line of male die is perpendicular to the axial line of initial billet, and this male die is marked as MD2.

The loading paths shown in Fig. 1 are different in sequence of male die movement. In loading path I, the billet is put along *x* axis, the *x* male die is MD1 and the *y* male die is MD2, the MD1s move at beginning and the MD2s move later. In loading path II, the billet is put along *y* axis, as shown in Fig. A 1; the *y* male die is MD1 and the *x* male die is MD2, the MD2s move at beginning

and the MD1s move later.

Two forming processes by loading path I and path II can be divided into three stages according to the contact state between male die and billet/workpiece. The first forming stage is the stage from the start to later moving male dies starting loading. The second forming stage is the stage from later moving male dies starting loading to die block of MD1 contacting with billet. The third forming stage is the stage from die block of MD1 contacting with billet to the end. The deformation pattern, the direction of metal flow, and the magnitude of velocity at different stages are different. The length of forming stage in different loading paths is also different.

### 3 Deformation characteristic under loading path I

In the forming process under loading path I, at the first forming stage, the deformation pattern by *x* male die, i.e. MD1, is forward extrusion (FE) and forward-lateral extrusion (FLE), as shown in Figs. 2(a) and (b); at the second forming stage, the main deformation pattern by *x* male die, i.e. MD1, is backward extrusion (BE), as shown in Figs. 2(c) and (d); at the third forming stage, the deformation pattern by *x* male die, i.e. MD1, is forward-lateral extrusion, as shown in Fig. 2(e); at the first to third forming stages, the deformation pattern by *y* male die, i.e. MD2, is backward extrusion, as shown in Figs. 2(c)–(e).

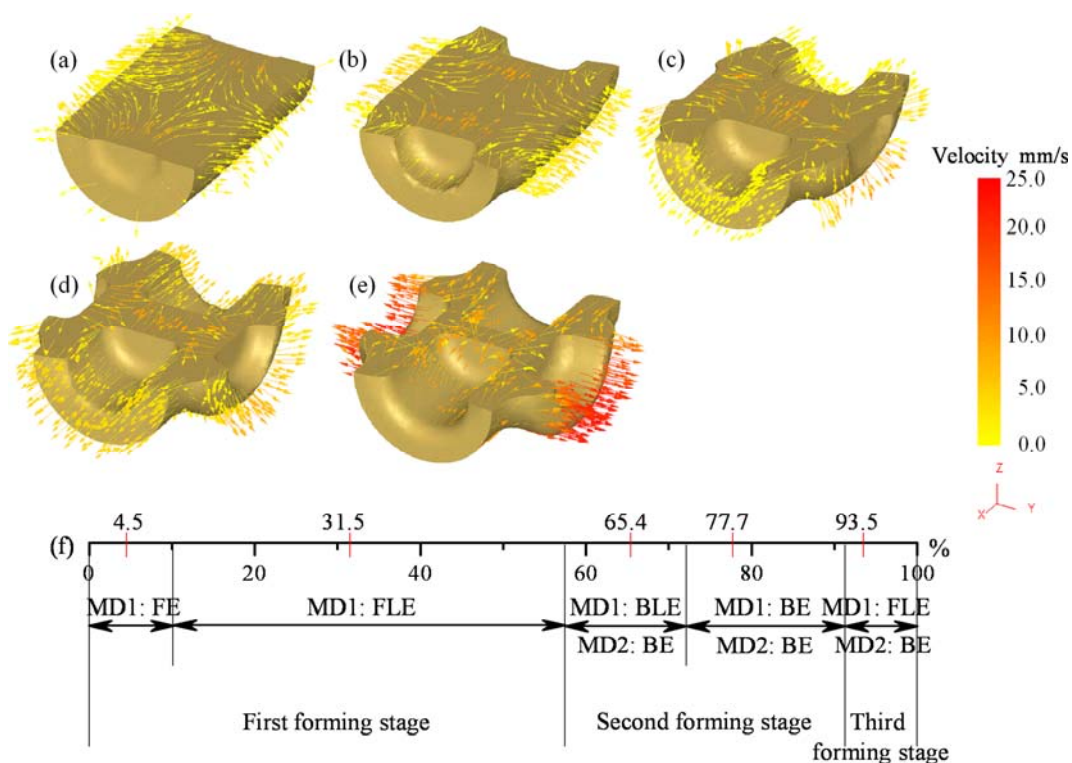


**Fig. 2** Typical velocity field and deformation pattern in the process under loading path I: (a) Forming ratio of 4.5%; (b) Forming ratio of 31.5%; (c) Forming ratio of 65.4%; (d) Forming ratio of 77.7%; (e) Forming ratio of 93.5%; (f) Deformation pattern

### 3.1 First forming stage

The first forming stage has a long time, which is more than half of the whole process, and the typical velocity fields are shown in Figs. 2(a) and (b). At the initial stage, the deformation only occurs in the zones around the rounded edge of punches. The metal in front of punch moves rigidly, and the metal surrounding the punch remains almost motionless. The end planes of billet keep the same position before forming, in other word, the length of billet along  $x$  axis is also 75 mm. At this time, the forward extrusion occurs in  $x$  axial cavity, and the metal surrounding the punch likes the container, and the velocity field is shown in Fig. 2(a). However, the time of the stage which has only forward extrusion is short, it is about one tenth of the whole process and less than one fifth of the first forming stage.

With the development of process, the constraint is applied to the billet by the intersecting line (as shown in Fig. A 1) of  $x$  and  $y$  axial cavities on the surface of female die. Then, the  $y$  axial cavity begins to be filled and the lateral extrusion appears, and the deformation pattern by  $x$  male die (MD1) is forward-lateral extrusion. The velocity field at this stage is shown in Fig. 2(b). At this time, not only the metal in front of punch but also the metal surrounding the punch moves along the loading direction of male die, and the  $x$  axial cavity likes the container. The  $x$  axial head face of billet does not keep a vertical plane, and the dishing around punch is caused, as shown Fig. 3. Later, the deformation is steadily achieved by forward-lateral extrusion. However, the phenomenon of dishing around punch becomes more and more notable due to the different velocity of metal flow between inner (closing to punch) and outer (closing to surface of female die). The inner velocity is greater than the outer velocity at the first forming stage, and thus the dishing on the head face is to reach maximum after the first forming stage. Figure 3(a) shows the geometry of billet/workpiece after the first forming stage. The length of workpiece along  $x$  axis is less than the initial length (i.e. 75 mm), and the outer and inner lengths reduce 0.5 and 6 mm, respectively. The length of workpiece along  $y$  axis increases 15 mm, but the  $y$  axial head face of workpiece shows a notable arched surface such as high in the center and low on the edges, as shown in Fig. 3(a), which is named short-filling in the present study. At the second forming stage, the metal flow into the edges of  $y$  axial head face is also inadequacy, as shown in Fig. 3(b), and the under-filling will be caused in the end.

### 3.2 Second forming stage

The second forming stage is about one third of the whole process, and the typical velocity fields are shown in Figs. 2(c) and (d). At this forming stage, the  $y$  axial cavity is slowly filled under the lateral extrusion by MD1

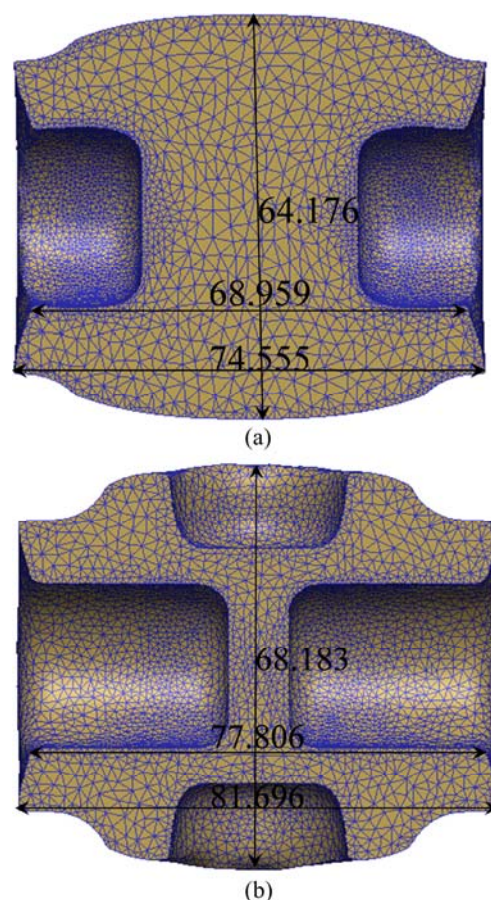


**Fig. 3** Shapes of head face under loading path I: (a) After the first forming stage; (b) After the second forming stage

and backward extrusion by MD2, and the length of workpiece along  $y$  axis only increases 4 mm, as shown in Fig. 3(b). The degree of dishing on the  $x$  axial head face reduces at this forming stage, but the dishing also exists and the difference between inner and outer length is more than 4 mm after the second forming stage, as shown in Fig. 3(b).

The resistance in  $y$  axial cavity increases because the  $y$  male dies are loaded. The metal surrounding the  $x$  axial punch changes its flowing direction. It flows into opposite loading direction of  $x$  male die, but the opposite flowing velocity is small. The metal in front of  $x$  axial punch mainly flows into  $y$  direction, and thus the deformation pattern by  $x$  male die (MD1) is backward-lateral extrusion, as shown in Fig. 2(c). With the  $y$  axial punch advancing, resistance in  $y$  axial cavity increases further. At the same time, the flowing velocity of metal surrounding the  $x$  axial punch increases, and the metal in front of  $x$  axial punch flows into  $x$  axial cavity, and then the deformation pattern by  $x$  male die (MD1) turns into backward extrusion, as shown in Fig. 2(d). When the fillet area between the punch and die block of  $x$  male die contacts with the workpiece, the flowing velocity along  $x$  axis begins to decrease.



### 3.3 Third forming stage

The length of workpiece along  $x$  axis is greater than requirement for forging after the second forming stage. Thus, the metal in  $x$  axial cavity is forced to flow along loading direction at the third forming stage, and then the flowing direction turns into opposite direction again. The deformation pattern by  $x$  male die (MD1) is forward-lateral extrusion and by  $y$  male die (MD2) is backward extrusion, and the typical velocity field at this forming stage is shown in Fig. 2(e).

At the close of the process, the metal in center zone of female die is constrained by 4 male dies, and then metal flows into  $y$  axial cavity via clear space between punches. Thus, the flowing velocity is large at the third forming stage, especially the  $y$  axial velocity which increases sharply. The dishing on the  $x$  axial head face disappears after the third forming stage.

## 4 Deformation characteristic under loading path II

In the forming process under loading path II, at the first forming stage, the deformation pattern by  $x$  male die, i.e. MD2, is backward-lateral extrusion (BLE), as shown in Fig. 4(a); at the second forming stage, the main deformation pattern by  $y$  male die (i.e. MD1) and  $x$  male die (i.e. MD2) is backward extrusion (BE), as shown in Fig. 4(b); at the third forming stage, the deformation pattern by  $y$  male die (i.e. MD1) is forward-lateral extrusion (FLE), and the deformation pattern by  $x$  male die (i.e. MD2) is backward extrusion, as shown in Fig. 4(c).

### 4.1 First forming stage

The first forming stage has a short time, which is less than one tenth of the whole process, and the typical velocity fields are shown in Fig. 4(a). No constraint is applied on the  $y$  axial head face of billet. The backward extrusion and lateral extrusion are both not very effective, and even the deformation behavior by lateral extrusion can be ignored. Thus, the change in length of workpiece along  $x$  or  $y$  axis is found to be insignificant.

### 4.2 Second forming stage

The second forming stage is about four fifths of the whole process, and the typical velocity fields are shown in Fig. 4(b). The cavities are mainly filled under backward extrusion pattern by  $x$  and  $y$  male dies, and the lateral extrusion by  $y$  male die can be ignored.

The filling velocity along  $x$  axis is much greater than that along  $y$  axis, and the filled metal in  $x$  axial cavity would undergo a severe plastic deformation. Similar to the loading path I, the dishing and short-filling defects also occur in the loading path II, but the short-filling presents another kind. The dishing around punch occurs on the head face in the direction ( $x$  axial direction for loading path I, and  $y$  axial direction for loading path II) which is parallel to the axial line of billet, as shown in region 1 in Fig. 5, but the difference of length between inner (closing to punch) and outer (closing to surface of female die) is small, and the dishing disappears after the second forming stage. The head face in the direction ( $y$  axial direction for loading path I, and  $x$  axial direction for loading path II) which is perpendicular to the axial line of billet shows a notable

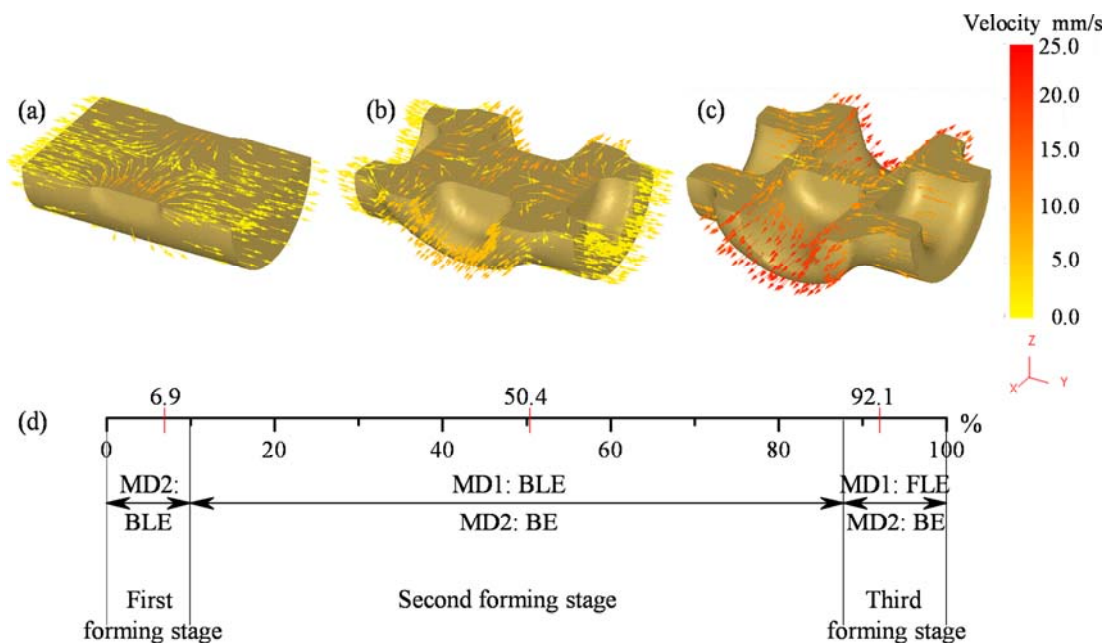


**Fig. 4** Typical velocity field and deformation pattern in the process under loading path II: (a) Forming ratio of 6.9%; (b) Forming ratio of 50.4%; (c) Forming ratio of 92.1%; (d) Deformation pattern

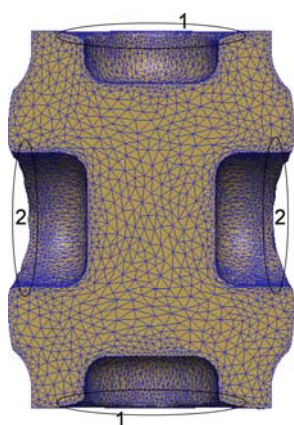


**Fig. 5** Shapes of head face under loading path II with forming ratio of 50%

concave arched surface such as low in the center and high on the edges, as shown in region 2 in Fig. 5.

### 4.3 Third forming stage

After the second forming stage, the difference of length along  $x$  or  $y$  axis between the reality for workpiece and requirement for forging is about  $\pm 5$  mm, and the differences along  $x$  and  $y$  axis are almost equal, and this is superior to that in loading path I. The length of workpiece along  $y$  axis is greater than requirement for forging after the second forming stage, thus the deformation characteristic in  $y$  axial cavity is similar to that in forward extrusion deformation. The typical velocity field at the third forming stage is shown in Fig. 4(c).

## 5 Comparison of both loading paths

FEM numerical simulations indicate that both loading paths I and II allow forming cross valve with correct shape, but there is a significant difference of cavity fill, forging load and metal flow between two groups due to notable different deformation characteristic under both loading paths.

In the forming processes under both loading paths, the dishing on the head face in the loading direction of MD1 ( $x$  male die for loading path I, and  $y$  male die for loading path II) and short-filling on the head face in the loading direction of MD2 ( $y$  male die for loading path I, and  $x$  male die for loading path II) are prone to occurrence. The dishing only disappears after the third forming stage in the process under loading path I, but the dishing will disappear at the second forming stage in the process under loading path II. The short-filling will be improved only at the third forming stage in the processes under both loading paths. It can be seen from Fig. 6 that the degree of short-filling on head face under loading path I is much larger than that under loading path II, and the under-filling may be caused under loading path I.

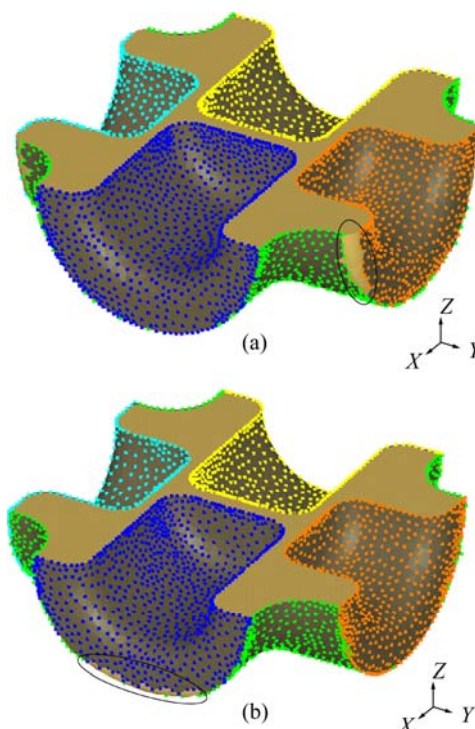


**Fig. 6** Contact conditions with dies of valve in the end of processes: (a) Loading path I; (b) Loading path II

Figure 7 illustrates the forging loading and max velocity of metal flow in the processes under loading paths I and II. In general, forging load of MD1 is larger than the forging load of MD2, especially at the third forming stage. It can be seen from Fig. 7 that the difference of forging load between two loading paths at the first and second forming stages is small, but that is notable at the third forming stage. ZHANG et al [17,18] also presented that there exists a notable difference of load between two loading paths at final stage, but the detailed reason is not described. The main reasons for this are that the  $x$  and  $y$  axial cavities are mainly filled under backward extrusion deformation at the first and second forming stages, and no constraint is applied on the  $x$  and  $y$  axial head faces of workpiece; but the cavity in loading direction of MD1 is filled under forward extrusion deformation at the third forming stage, and the resistance in the cavity increases sharply; and a notable difference of constraint condition between two loading paths at the third forming stage is caused by the different deformation patterns at the first and second stages.

In the process under loading path I, the difference of length along  $x$  axis between the reality for workpiece and requirement for forging is much less than that along  $y$  axis. Thus, the resistance in  $x$  axial cavity is much larger than the resistance in  $y$  axial cavity. Then, the maximum load of  $x$  axial male die is much larger than that of  $y$  axial male die, and the discrepancy is about 40%.

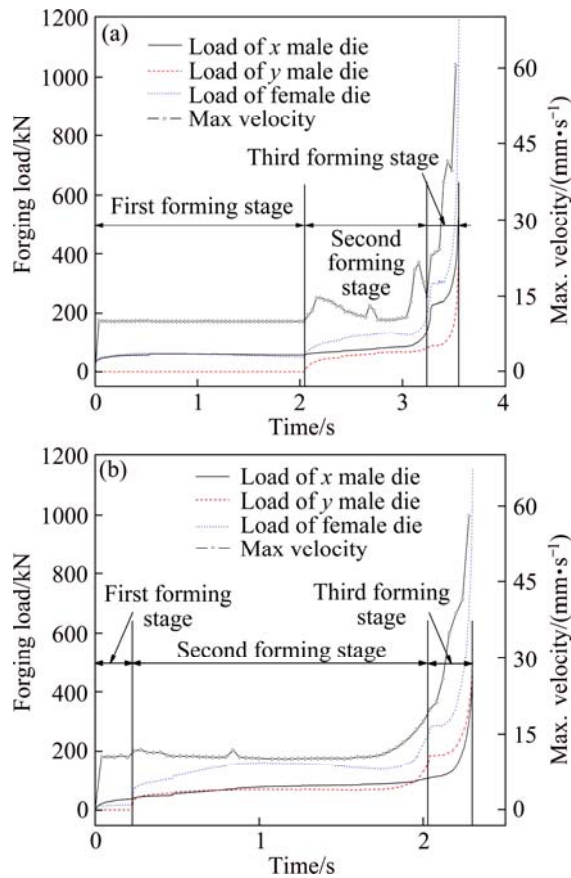


**Fig. 7** Forging load and maximum velocity at FEM node in process: (a) Loading path I; (b) Loading path II

In the process under loading path II, the differences of length along  $x$  and  $y$  axis between the reality for workpiece and requirement for forging are almost equal. Thus, the resistances in  $x$  and  $y$  axial cavities are about the same. Then, the maximum loads of  $x$  and  $y$  axial male dies are also about the same, and the discrepancy is less than 8%.

The first forming stage is more than half of the whole process under the loading path I, and the cavity fill at this forming stage is not ideal. More than half of the whole cavity fill for the cavity in the loading direction of MD2 ( $y$  male die) is achieved at the third forming stage, which is less than one eleventh of the whole process under the loading path I. However, the first and second forming stages are both about one tenth of the whole process under the loading path II. The most of forming process is at the second forming stage, and the most of cavity fill for  $x$  and  $y$  axial cavities will be achieved at this forming stage. Comparing to the loading path I, the cavity fill behavior under loading path II is more stable, and the changes in the velocity of metal flow and load of male die are more even.

In the process under loading path II, the maximum velocity at FEM node varies smoothly, and the maximum velocity almost keeps a constant at the first and second

forming stages, and the maximum velocity becomes steadily increasing in the end of second forming stage, as shown in Fig. 7(b). However, in the process under loading path I, the maximum velocity at FEM node begins to fluctuate at the second forming stage, and the maximum velocity increases sharply at the third forming stage, as shown in Fig. 7(a).

The metal flow on the head face of workpiece is also very complex. In order to research the metal flow characteristic on the head face of workpiece, 3 points on the  $x$  axial head face and 3 points on  $y$  axial head face are chosen, and the 6 points are expressed as  $P_1$  to  $P_6$ . The positions of the  $P_1$  to  $P_6$  before loading and after the forming process are shown in Fig. 8. The positions of  $P_1$  and  $P_2$  are symmetrical about the axial line of MD1, and the positions of  $P_4$  and  $P_5$  are symmetrical about the axial line of MD2. The velocities at  $P_1$  to  $P_6$  in the forming process can be obtained by FEM simulation, and the velocity of metal flow on the head face of workpiece can be expressed as follows:

$$v_{HF_x} = \begin{cases} \text{Loading path I: } (v_{P_1} + v_{P_2} + 2v_{P_3})/4 \\ \text{Loading path II: } (v_{P_4} + v_{P_5} + 2v_{P_6})/4 \end{cases} \quad (1)$$

$$v_{HF_y} = \begin{cases} \text{Loading path I: } (v_{P_4} + v_{P_5} + 2v_{P_6})/4 \\ \text{Loading path II: } (v_{P_1} + v_{P_2} + 2v_{P_3})/4 \end{cases} \quad (2)$$

where  $v_{HF_x}$  and  $v_{HF_y}$  are the velocities on  $x$  and  $y$  axial head face, respectively. If  $v_{HF_i} > 0$  ( $i=x, y$ ), then the flowing direction is the loading direction of  $i$  male die; if  $v_{HF_i} < 0$  ( $i=x, y$ ), then the flowing direction is the opposite loading direction of  $i$  male die.

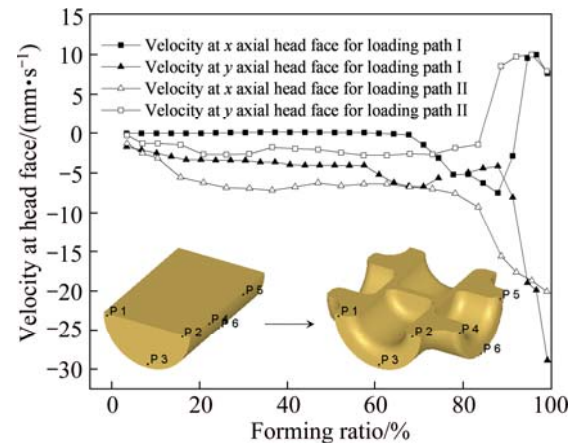


**Fig. 8** Velocity of metal flow at head face

It can be seen from Fig. 8 that the velocity on the head face in the direction ( $y$  axial direction for loading path I and  $x$  axial direction for loading path II) perpendicular to the axial line of initial billet is less than 0 from beginning to the end of process. However, the flowing direction of velocity on the head face in the direction ( $x$  axial direction for loading path I, and  $y$  axial



direction for loading path II) parallel to the axial line of initial billet will turn into opposite direction in the process. In the process under loading path I, the flowing direction of velocity on  $x$  axial head face turns twice, and the value of velocity on  $y$  axial head face changes sharply at the third forming stage. In the process under loading path II, the flowing direction of velocity on  $y$  axial head face only turns once, and the change in the velocity is also more even than that under loading path I.

The essential reason for the difference between both loading paths is that the deformation behavior caused by male die under different loading paths is different. The velocity of metal flow increases, decreases, and turns direction during the process, and the value, degree and time of these changes are different for loading paths I and II, and then the cavity fill, forging load and field variables under loading paths I and II show a notable difference.

## 6 Conclusions

1) The multi-way loading forming process of cross valve under both loading paths can be divided into 3 forming stages according to the contact state between male die and billet/workpiece. There exist 4 deformation patterns in the forming process such as forward extrusion, backward extrusion, forward-lateral extrusion, and backward-lateral extrusion.

2) During the forming process, two defects would occur on the head face of workpiece, such as the dishing around punch of MD1 and the short-filling on the head face loading by MD2. Through adjusting loading path, the degree of the defects can be reduced, and the defects can be improved and may even disappear.

3) In order to improve the forming quality, turning direction of metal flow during process should be reduced or be avoided, and forward extrusion deformation by MD1 at the third forming stage should also be reduced or be avoided.

## Appendix

### Finite element model in Ref. [17]

A coupled thermo-mechanical finite element model of the process of multi-way loading for cross valve was developed under DEFORM-3D environment, as shown in Fig. A 1. In order to reduce computational time and save storage capacity, the half of billet and male dies was modeled. The nodes at the symmetry plane were restrained in the normal direction of symmetry plane. The geometric models of billet and dies were built through CAD software, and then were meshed and assembled through DEFORM-3D.

Local mesh densification and automatic remeshing

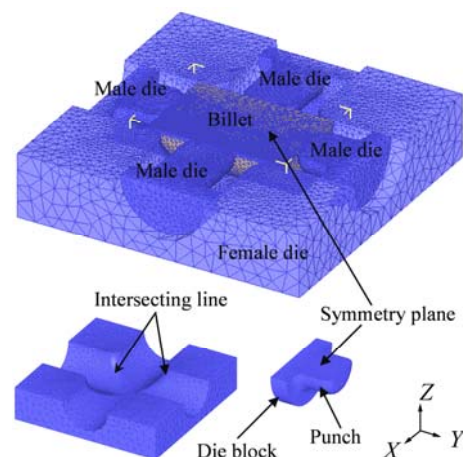


**Fig. A 1** Finite element model of cross valve multi-way loading forming

technology were used to improve the computational efficiency and avoid mesh distortion. The initial meshes in dies were not homogeneous, being coarser beyond the die-billet interface.

The material of valve was aluminum alloy 7075 and the material of dies was H-13 hot die steel, and the material properties of the billet and the die came from the material library in DEFORM-3D. The von Mises yielding criteria and shear friction model were employed in the model.

The thermal conductivity of aluminum alloy is much greater than that of die steel, and aluminum alloy is very sensitive to deformation temperature. So the die was preheated up to close initial temperature of billet.

## References

- [1] XIA J, WANG Y. A study of a die set for the multiway die forging of pipe joints [J]. *International Journal of Machine Tools and Manufacture*, 1991, 31(1): 23–30.
- [2] GONTARZ A. Forming process of valve drop forging with three cavities [J]. *Journal of Materials Processing Technology*, 2006, 177: 228–232.
- [3] ZHANG Da-wei, YANG He, SUN Zhi-chao. Research status of multi-way loading near-net shape forming [J]. *Journal of Netshape Forming Engineering*, 2009, 1(1): 39–46. (in Chinese)
- [4] YANG H, ZHAN M, LIU Y L, XIAN F J, SUN Z C, LIN Y, ZHANG X G. Some advanced plastic processing technologies and their numerical simulation [J]. *Journal of Materials Processing Technology*, 2004, 151: 63–69.
- [5] ROWE G W, STURGESS C E N, HARTLEY P, PILLINGER I. *Finite-element plasticity and metalforming analysis* [M]. Cambridge: Cambridge University Press, 1991.
- [6] LIN Y C, CHEN M S, ZHONG J. Numerical simulation for stress/strain distribution and microstructural evolution in steel during hot upsetting process [J]. *Computational Materials Science*, 2008, 43: 1117–1122.
- [7] HE You-feng, XIE Shui-sheng, CHENG Lei, HUANG Guo-jie, FU Yao. FEM simulation of aluminum extrusion process in porthole die with pockets [J]. *Transactions of Nonferrous Metals Society of China*, 2010, 20(6): 1067–1071.



- [8] HE Zhao, WANG He-nan, WANG Meng-jun, LI Guang-yao. Simulation of extrusion process of complicated aluminium profile and die trial [J]. Transaction of Nonferrous Metals Society of China, 2012, 22(7): 1732–1737.
- [9] ZHANG Shi-hong, SUN Cheng, WANG Zhong-tang. Finite element simulation on press forging of magnesium alloy AZ31 sheets [J]. Transactions of Nonferrous Metals Society of China, 2008, 18(s1): s269–s272.
- [10] HUANG L, YANG H, ZHAN M, HU L J. Forming characteristics of splitting spinning based on behaviors of roller [J]. Computational Materials Science, 2009, 45: 449–461.
- [11] LIU Gang, ZHOU Jie, DUSZCZYK J. Process optimization diagram based on FEM simulation for extrusion of AZ31 profile[J]. Transactions of Nonferrous Metals Society of China, 2008, 18(s1): s247–s251.
- [12] GUO Qiang, LIU Yu-li, YANG He. Field-variable distribution laws of the blade with a damper platform during multi-directional forging process [J]. Materials Science & Technology, 2010, 18(2): 159–163. (in Chinese)
- [13] SUN Z C, YANG H, GUO X F. Modelling of microstructure evolution in AISI 5140 steel triple valve forming under multi-way loading [J]. Steel Research International, 2010, 81(9): 282–285.
- [14] CHENG M, ZHANG Z M. Metal flow behavior on the non-uniform wall thickness three-way valve extrusion [J]. Materials Science Forum, 2008, 575–578: 328–333.
- [15] ZHANG D W, YANG H, SUN Z C. 3D-FE modelling and simulation of multi-way loading process for multi-ported valve [J]. Steel Research International, 2010, 81(3): 210–215.
- [16] XU Ji-sheng. Study on metal flow in multi-ram forging process of equal diameter tee joint [J]. Forging & Stamping Technology, 2002(4): 11–14. (in Chinese)
- [17] ZHANG Da-wei, YANG He, SUN Zhi-chao. Finite element simulation of aluminum alloy cross valve forming by multi-way loading [J]. Transactions of Nonferrous Metals Society of China, 2010, 20(6): 1059–1066.
- [18] ZHANG Da-wei, SUN Zhi-chao, YANG He. Simulation analysis of influences of forming parameters on cross valve multi-way loading process [J]. Forging & Stamping Technology, 2010, 35(3): 148–152. (in Chinese)

## 基于有限元法的铝合金四通阀 多向加载成形过程中的变形特征分析

张大伟<sup>1</sup>, 赵升吨<sup>1</sup>, 杨 合<sup>2</sup>

1. 西安交通大学 机械工程学院, 西安 710049;

2. 西北工业大学 材料学院, 西安 710072

**摘 要:** 采用数值模拟方法, 研究 7075 铝合金四通阀类零件在多向加载成形条件下成形过程中的材料变形特征。结果表明: 四通阀多向加载成形过程中存在正挤、反挤、正挤和侧挤复合、反挤和侧挤复合等 4 种变形模式。在不同成形阶段, 表现出的变形模式依赖于加载路径。一般在变形初期会发生正挤或反挤的变形行为; 在变形中期以反挤变形模式为主; 在变形终期一般会发生反挤、正挤和侧挤复合变形模式。为提高型腔填充稳定性和减少成形缺陷, 在变形初期和中期, 应增加侧挤变形行为; 在变形终期应减少或避免正挤变形行为。

**关键词:** 四通阀体; 多向加载; 变形行为; 材料流动; 铝合金; 有限元; 数值模拟

(Edited by Chao WANG)